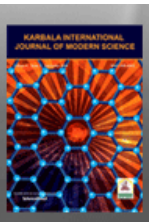

Karbala International Journal of Modern Science

Volume 8 | Issue 2 Article 10

Efficient removal of common organic pollutants from water by Zn-doped TiO2 nanoparticles with different applications

Khaled Elgendy
Chemistry Department, Faculty of Science, Zagazig University, Zagazig, Egypt

Ibrahim Elmehasseb
Chemistry Department, Faculty of Science, Kafrelsheikh University, Kafrelsheikh, Egypt

Saleh Kandil
Chemistry Department, Faculty of Science, Zagazig University, Zagazig, Egypt, abosalah281182@gmail.com

Efficient removal of common organic pollutants from water by Zn-doped TiO2 nanoparticles with different applications

Abstract

Water purification via adsorption without energy consumption was considered a green process. Zn-doped TiO2 nanoparticles were fabricated by the Sol-gel method and characterized by different analysis techniques. Zinc doping of TiO2 increases the surface area to 26.7m2g-1 with adsorption results, 75.1%, 71.1%, and 68.2% for methylene blue, ofloxacin, and SLS, respectively. Variable affecting factors on adsorption have been studied. The adsorption behavior fitted with Langmuir and Freundlich equations than Temkin isotherm, indicating the preferred heterogeneous adsorption at equivalent adsorbent sites. The application of nanoparticles in many synthetic specimens of pollutants gave excellent removal results, which exceeded 75% of detoxification.

Keywords

Nanoparticles; Zn doping, TiO2; adsorption, sol-gel, characterization, synthetic laboratory specimens, isotherm

RESEARCH PAPER

Efficient Removal of Common Organic Pollutants from Water by Zn-doped TiO_2 Nanoparticles with Different Applications

Khaled Elgendy [a], Ibrahim Elmehasseb [b], Saleh Kandil [a,*]

[a] Chemistry Department, Faculty of Science, Zagazig University, Zagazig, Egypt
[b] Chemistry Department, Faculty of Science, Kafrelsheikh University, Kafrelsheikh, Egypt

Abstract

Water purification via adsorption without energy consumption was considered a green process. Zn-doped TiO_2 nanoparticles were fabricated by the Sol−gel method and characterized by different analysis techniques. Zinc doping of TiO_2 increases the surface area to 26.7m^2g^{-1} with adsorption results, 75.1%, 71.1%, and 68.2% for methylene blue, ofloxacin, and SLS, respectively. Variable affecting factors on adsorption have been studied. The adsorption behavior fitted with Langmuir and Freundlich equations than Temkin isotherm, indicating the preferred heterogeneous adsorption at equivalent adsorbent sites. The application of nanoparticles in many synthetic specimens of pollutants gave excellent removal results, which exceeded 75% of detoxification.

Keywords: Nanoparticles, Zn doping, TiO_2, Adsorption, Sol−gel, Characterization, Synthetic laboratory specimens, Isotherm

1. Introduction

One of the most current serious challenges scientists face worldwide is water pollution. Various sources lead to the contamination of water by multiple pollutants. The most affecting factor in water is the industry's continuous progress in different fields. Industrial wastes lead to elevated levels of other contaminants, resulting in water contamination and high toxicity parameters [1−5]. One of the heaviest industries is the textile fabrication or the paint industry. The utilization of various dyes led to the high concentration of these organic compounds in wastewater. These complex compounds have extremely toxic effects when accumulated in a high percentage of living cells because of their continuous discharge in an aquatic environment, causing various skin infections respiratory system and can cause cancer.

Various pharmaceutical products like antibiotics were another type of common pollutants. Variable antibiotics have been manufactured to face different diseases which attack both animals and humans [6−10]. By that time, the continuous consumption of antibiotics and subsequent release of their wastes into the environment through the ecosystem caused their accumulation in living organisms to high and dangerous levels [11−16]. This problem affects the quality of water and the medical effect of these drugs and generates microbial resistance [17−20].

The most common compounds which are used everywhere in different products are surfactants. They are used in detergents for toothpaste, shampoos, shaving foams, floor cleaners, clothes, etc. Surfactants are also used to fabricate various types of cosmetics for skin and hair care products [21−23]. We have to imagine the amounts of these complex compounds released through water without

Received 25 November 2021; revised 31 January 2022; accepted 5 February 2022.
Available online 1 May 2022.

* Corresponding author at:
E-mail address: abosalah281182@gmail.com (S. Kandil).

https://doi.org/10.33640/2405-609X.3226

subsequent several treatment stages. The shortage in the treatment of water from these accumulated amounts of toxic compounds could lead to harmful and horrible results. These complex products are not biodegradable and accumulate in water and subsequently in a living organism's cell, leading to several types of diseases and dangerous and carcinogenic effects [24–33].

Variable analytical techniques have been employed to remove these common pollutants from water in different treatment processes such as chemical coagulation, sedimentation, reverse osmosis, and electrodialysis [34–36]. Recently, nanoparticles have been employed in wastewater treatment via adsorption as a green and energy-saving purification without any subsequent harmful effects of energy consumption [36–44]. Bare TiO_2 and zinc-doped TiO_2 nanoparticles have been employed in this field and have given excellent results. These nanoparticles have been synthesized by a sol–gel method characterized by its simplicity and can be carried out at ambient temperature with few procedure needs. Doping of TiO_2 by zinc species improves its adsorption properties. This process involves the sharing of electrons between an adsorbent and an adsorbate, and a resulting thin layer of chemical compounds is formed [5,45–48].

Adsorption is an essential class of catalysis that is preferred more than many other chemical techniques for wastewater treatment. Different types of common adsorbents are widely used in toxin removals like clay, activated carbon, graphene, and different metal oxides [49–51]. TiO_2 and zinc-doped TiO_2 nanoparticles can effectively absorb various pollutants because they are characterized by their high porosity and enhanced surface area.

It is known that the applicability of different nanomaterials in wastewater treatment in light via photocatalytic degradation or sonophotocatalytic degradation processes [52–57]. But this work discusses the high performance of Zn-doped TiO_2 than bare TiO_2 in removing organic compounds in the dark without any assisting preparations or procedures with very little amounts of nanomaterial and free of energy consumption.

The choice of toxins in this study, methylene blue, ofloxacin, and sodium lauryl sulfate (SLS), is a desire to prove their possible application in the widespread treatment of water from common pollutants and the ability of the nanoparticles of simultaneous removal of cationic and anionic compounds from water [58,59]. The study involved the successful application of Zn-doped TiO_2 nanoparticles on several synthetic samples of common pollutants.

The chemical structure of selected pollutants in this article (a) methylene blue, (b) ofloxacin, and (c) sodium lauryl sulfate (SLS) is represented as follows in the scheme (1):

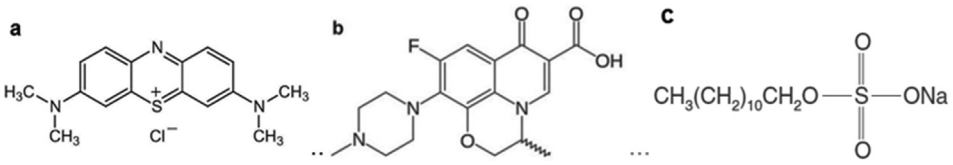

Scheme 1. Chemical structure for the selected pollutants.

2. Experimental

2.1. Chemical precursors, solvents, and solid materials

The precursors of titanium and zinc were Titanium (IV) butoxide ($Ti(OCH_2CH_2CH_2CH_3)_4$) grade 97%, and Zinc citrate dihydrate ($(C_6H_5O_7)_2Zn_3 \cdot 2H_2O$ respectively, methylene blue (MB) powder [$C_{16}H_{18}ClN_3S$], Cetyltrimethylammonium bromide (CTAB) [$(C_{16}H_{33})$ N $(CH_3)_3$]Br and Sodium lauryl sulfate (SLS) [CH_3 $(CH_2)_{11}OSO_3Na$)], sodium hydroxide (NaOH) obtained from Sigma–Aldrich. Ofloxacin ($C_{18}H_{21}ClFN_3O_4$) was obtained from Loba Company (India). Absolute ethanol ≥99.9%, glacial acetic acid (CH_3COOH), and hydrochloric acid (HCl) were obtained from Sigma–Aldrich and double-distilled water.

Other chemical materials as interfering species were utilized without treatment and used as received.

2.2. TiO_2 sol–gel preparation

Titanium dioxide nanoparticles have been synthesized via the sol–gel technique as the following steps: 20 ml titanium precursor (Titanium (IV) butoxide) was stirred with 40 ml of 99.9% ethanol followed by adding of 4 ml glacial acetic acid with stirring for 30 min at 1000 rpm. This solution was considered solution A.

Solution B involved the dissolution of 4 g of CTAB powder was dissolved in 100 ml of double-distilled water at 70 °C using another flask with stirring for 10 min [45]. Solution A was added to B dropwise with strong stirring to avoid agglomeration. The vigorous stirring continued for 12 h. The formed solid particles were isolated by centrifugation at 6000 rpm for 5 min and removing excess solution. The precipitate was washed several times with double distilled water and ethanol. The resulting nanoparticles were dried at 70 °C for 6 h, then calcined at 450 °C for 4 h with a 5 °C/min ramp.

2.3. Preparation of Zn doped -TiO_2 nanoparticles

Considering the previous sol–gel preparation of TiO_2 nanoparticles, Zinc citrate dihydrate $(C_6H_5O_7)_2Zn_3 \cdot 2H_2O$ was dissolved in double-distilled water, corresponding to about 5% wt Zn to the total amount of TiO_2. The solution has been vigorously stirred for 1 day. The resulting precipitate was filtered, dried at 70 °C of obtaining nanoparticles of Zn doped -TiO_2 at 70 °C for 6 h and calcined at 450 °C for 6 h and 5 °C/min ramps.

2.4. Characterization

TiO_2 and Zn doped -TiO_2 chemical structure was investigated by FTIR (FT/IR-6800 JASCO Japan). XRD phase pattern (Lab XRD-6000 SHIMADZU Japan) to study particle size different structure phases with a scan rate of 8° min^{-1}. SEM surface textures were provided by (JSM IT 100 JEOL Japan). The shape and size of nanoparticles were evaluated using HR-TEM (JOEL 2000). UV spectrophotometer (UV-2450 SHIMADZU Japan) is used to measure the absorbance of the pollutants after being subjected to treatment. The surface uptake performance of nanoparticles has been studied by removing three common toxic pollutants (methylene blue dye, ofloxacin antibiotic, and the detergent sodium lauryl sulfate (SLS).

2.5. Adsorption procedures of pollutants

Bare TiO_2 and Zn doped-TiO_2 nanoparticles have been utilized in the adsorption of pollutants by different doses of adsorbent (3, 5, 7, 10, 15, and 20 mg) and variable initial concentration range of dye, drug, and surfactant (3–20 μg/ml). The pH factor was studied using different pH solutions of values (1, 3, 5, 7, 9, and 12). The effect of temperature was examined in the range of (20–45 °C). The absorbance values were measured at 663 nm and took a reading every 5 min during continuous stirring with nanoparticles. The same parameters were studied for the other pollutant and the removal of ofloxacin, and SLS was spectrophotometrically recognized at 284 nm and 247 nm, respectively, as seen in Table 1.

The effect of interfering species in total solution was examined using "glucose, TiO_2, KCl, Diclofenac sodium" as interfering pollutants at higher concentrations 50-fold than that of dye, drug, and detergent. These measurements were carried out when the preparation of 10 ml of 10 μg/ml of methylene blue, ofloxacin, and 200 μg/ml SLS was prepared, followed by taking the blank solution absorbance. After stirring the interfering component for 5 min, another absorbance value was measured.

2.6. Applications in water samples

After studying all of the above influencing factors, it was essential to give a vital application through the treatment of some artificial laboratory samples. These samples were synthesized at varying concentrations of these different complex pollutants. Then modified Zn doped -TiO_2 nanoparticles were introduced into the treatment process and stirred with 10 ml of each wastewater sample. Each sample was stirred for 5 min at 1500 rpm and then filtered, followed by absorbance measurement of the resultant clear solution by UV–visible spectrophotometer, at 663 nm for methylene blue, 284 nm for ofloxacin, and at 247 nm for the anionic detergent.

3. Results and discussion

3.1. Characterization of the fabricated nanoparticles TiO_2 and Zn doped -TiO_2

3.1.1. Fourier transform infrared spectroscopy (FTIR)

The FTIR analysis of doped and undoped TiO_2 nanoparticles represents a variable specific vibration

Table 1. Experimental conditions for dye, drug, and surfactant adsorption.

Experimental conditions	
Parameter	Condition
Solution volume (ml)	10 ml
Stirring speed (rpm)	1500 rpm
Adsorbent dose (mg)	3–20 mg
Pollutant initial concentration (μg/ml)	3–20 μg/ml
pH	1–12
Temperature °C	20–45 °C
Wavelength (nm)	663 nm for dye 284 nm for drug 247 nm for surfactant
Frequent measurement	Every 5 min

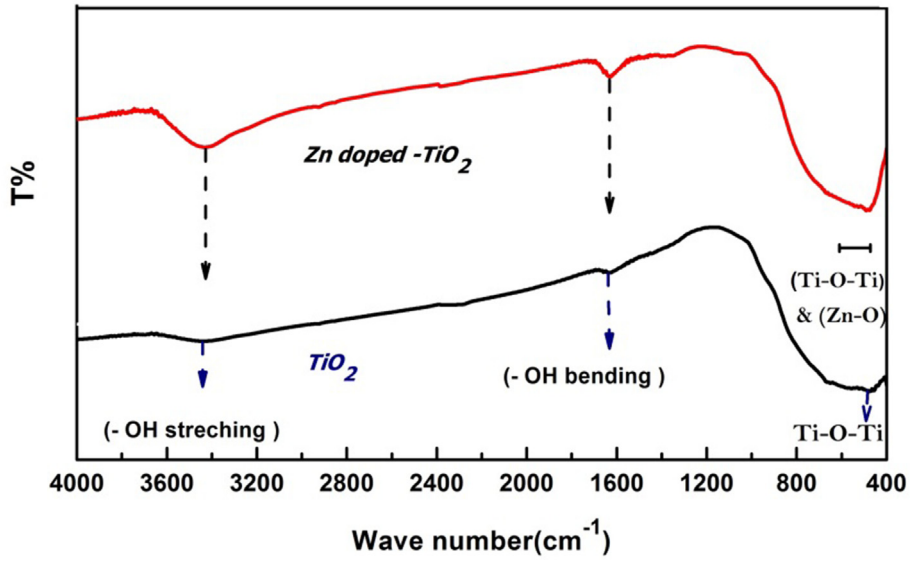

Fig. 1. FTIR curves of TiO_2 and Zn doped -TiO_2.

and stretching bands which can be illustrated as follows: a clear peak at 495 cm^{-1} attributed to the bending vibration mode of (Ti−O−Ti). For the doped nanoparticles, it was noticed that the doping process of TiO_2 by zinc species causes the modification of the spectrum shape of range (460−650) cm^{-1} due to the change in nanoparticles structure and resulted in the appearance of stretching band of (Zn−O) at 470 cm^{-1}. The hydroxyl group has a peak at 1650 cm^{-1} representing the bending vibration mode of adsorbed water at the surface of nanoparticles.

Broadband between (3400−3650) cm^{-1} refers to stretching vibration of O−H hydroxyl groups as a result of the hydrolysis of titanium precursor by alcohol in addition to the reaction between nanoparticle surface and water. From the FTIR spectrum in Fig. 1, it is clear that the increase in the intensities of both stretching and bending peaks at (1650, between 3400 and 3600) results from successful zinc doping in the crystal lattice of TiO_2 [5].

3.1.2. X-ray diffraction characterization (XRD)

The nanoparticles fabricated via the sol-gel technique were mainly anatase phase, proved by XRD patterns in Fig. 2. For TiO_2 and Zinc doped -TiO_2 nanoparticles. The doping process affected particle sizes to smaller sizes by a few zinc species and prevented the transforming anatase phase.

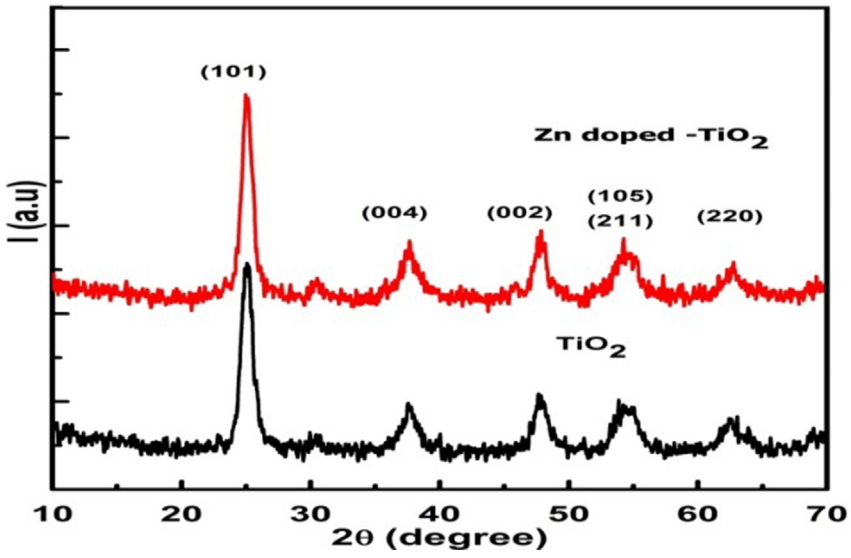

Fig. 2. XRD of TiO_2 and Zn doped -TiO_2 nanoparticles.

A clear peak at 25.2° refers to the anatase phase, in addition to the smaller peaks 37.6°, 48.0°, 54.9°, and 62.6°. The patterns of TiO_2 and Zn doped -TiO_2 are close to each other due to the few doped impurities, but Zn species gave more stabilization to the anatase phase because of its electronic configuration, in addition to the particle sizes that were calculated by Scherer's equation have average particle sizes for titanium dioxide were 20.2 nm and 29.5 nm, however, gave lower values of 19.4 nm and 25.1 nm for Zn-doped TiO_2 [5].

3.1.2.1. Morphological and characterization. Each transmission and scanning electron microscope provided with (EDX) gives valuable feedback and sufficient study about the material's surface and the

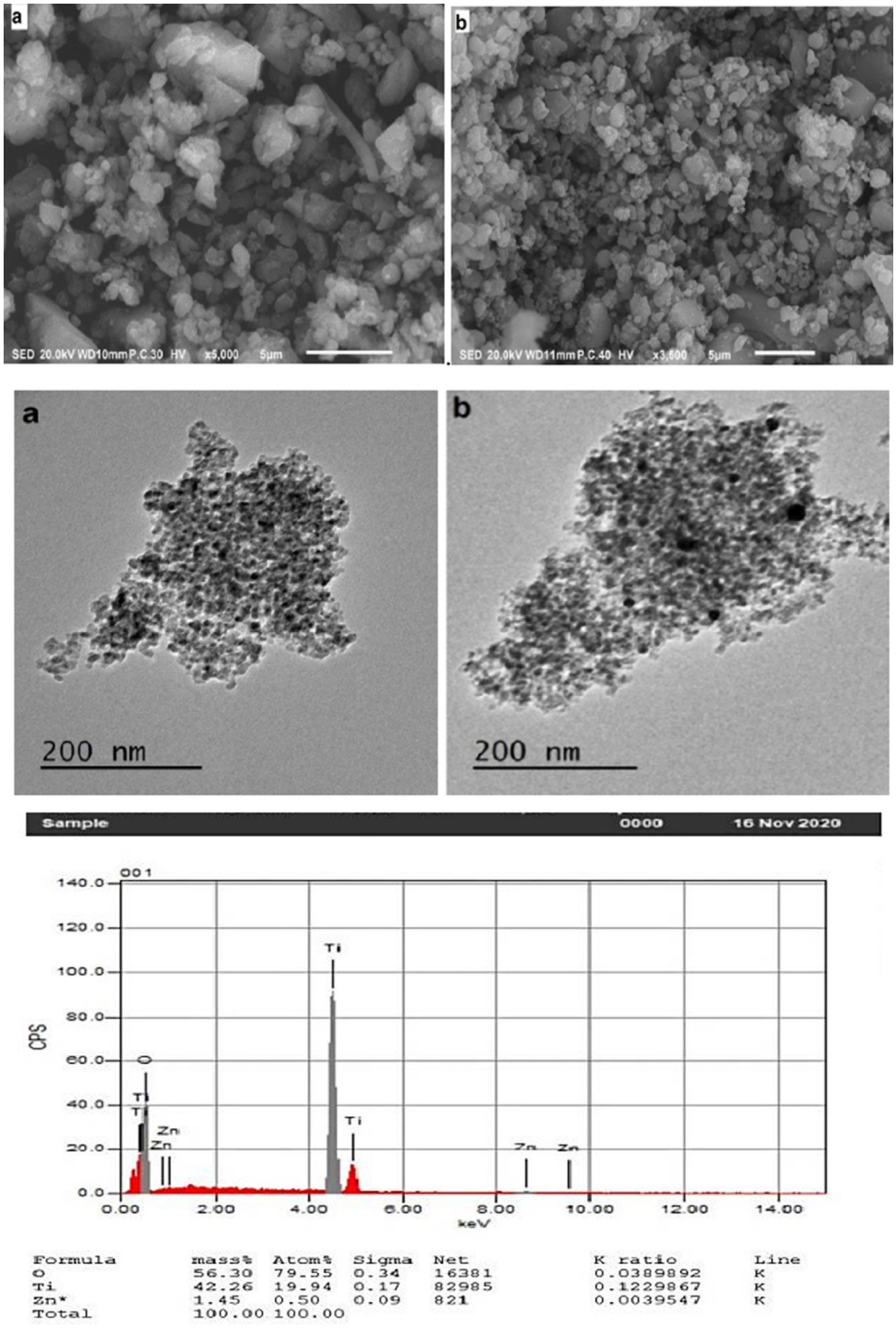

Fig. 3. (a, b) SEM and TEM images for TiO_2 and Zn doped -TiO_2 with EDX.

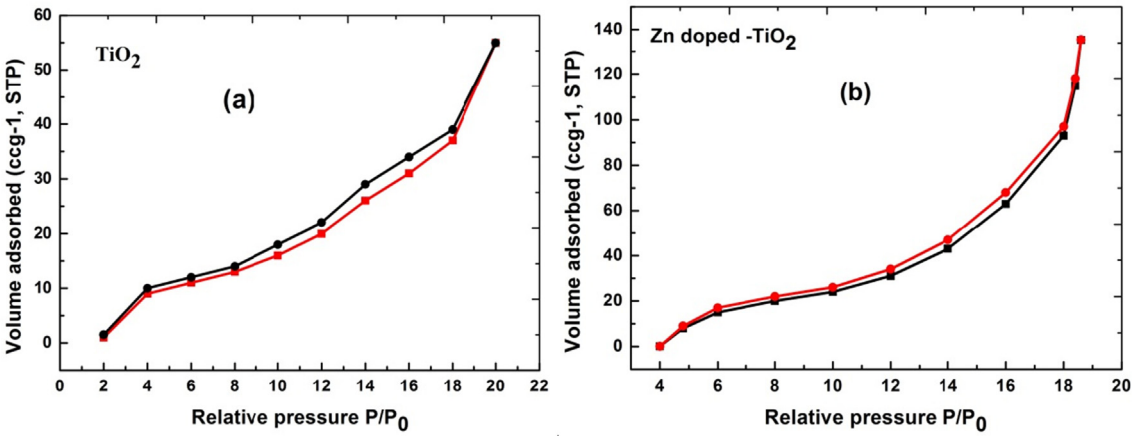

Fig. 4. N_2 adsorption/desorption isotherms for (a) TiO_2 and (b) Zn doped -TiO_2.

synthesized nanoparticles' morphology and shape. The resultant synthesized modified nanomaterial by doping` with different species can be examined by (EDX) studies. EDX evaluated the successful doping of TiO_2 nanoparticles by zinc in this work. As seen from Fig. 3 (a, b), most of the particles have a mainly spherical shape with nearly a similar particle size, but the doped nanoparticles have smaller sizes as a result of doping by species with smaller ionic radii like zinc, which replace the titanium ions in the crystal lattice, causing their retraction to lower dimensions.

TiO_2 nanoparticles have a size range (22–30 nm) that matches XRD results. Doping decreases this size range, which became between 16 nm and 27.5 nm due to distortion of crystal lattices with more restriction [46,47].

3.1.3. BET surface area analysis

N_2 adsorption–desorption measurements measured the synthesized nanoparticles TiO_2 and zinc doped TiO_2 to study BET surface area and pore radius. The determined values were 15.512 m^2g-1 and 17.623 nm for TiO_2 and 26.756 m^2g^{-1} and 1.911 nm for zinc-doped TiO_2, illustrated by Fig. (4) a, b, and Table 2.

From the measured data, it is clear that the dramatic modification of surface area and porosity with increasing the number of pores for Zn-doped TiO_2 more than bare TiO_2 explains the better adsorption properties for modified nanoparticles [60].

3.2. Adsorption of pollutants onto modified TiO_2

Variable removal applications have been carried out via adsorption technique using TiO_2 and Zn doped -TiO_2 nanoparticles to examine their ability to remove different toxins from wastewater and test the efficiency of the modified surface. The examined applications involved the adsorption of the most common pollutants, which are present everywhere and used continuously for different purposes like the example of dyes (methylene blue), an example of drugs (ofloxacin), and an example of surfactants (Sodium lauryl sulfate (SLS)). Calculating the removal% after equilibrium between the pollutants (methylene blue, ofloxacin, and SLS) and the surface of the nanoparticles (Bare $TiO_2$and Zn-doped-TiO_2) according to the following equation (1):

$$Removal\% = \left(\frac{C_i - C_e}{C_i}\right) \times 100 \quad (1)$$

where (C_i), (C_e) is the initial concentration of the pollutant and at equilibrium (mg L^{-1}). These calculations can be computed from data on absorbance. The initial concentration and concentration values at equilibrium can be replaced by the values of initial absorbance (A_i) and absorbance at equilibrium (A_e).

3.2.1. Removal results of pollutants by adsorption

Removal of toxins from wastewater was examined by different doses of TiO_2 and Zn doped -TiO_2 (5, 7,

Table 2. N_2 adsorption–desorption measurements for TiO_2 and zinc doped TiO_2.

Sample	Surface area (m^2g^{-1})	Pore radius (nm)	Pore volume (Cm^3g^{-1})
TiO_2	15.512	17.623	0.2925
Zn doped -TiO_2	26.756	1.911	0.1381

10, 15, and 20 mg) in solutions with different pH values (1, 3, 5, 9, and 12). Different initial concentrations of the organic dye (3, 5, 7, 10, 15 ppm) have been examined. The effect of temperature was studied at a range of (20–45 °C) in addition to the time factor. From the plotted curves (Fig. 5), it is clear that the increasing of nanomaterial enhances the adsorption results for all pollutant removal due to more surface area and the increasing of available pores and active sites. For methylene blue, the removal was enhanced in a basic medium more than an acidic medium due to the increase of negatively charged sites on the adsorbent surface as methylene blue is a cationic dye. Ofloxacin has both basic and acidic groups in its chemical structure, which causes different behavior towards the change of the medium pH range. Removal of the ofloxacin drug gave the best results between weak, acidic, and weak basic mediums and became quite stable in a neutral medium. The best removal range of pH for

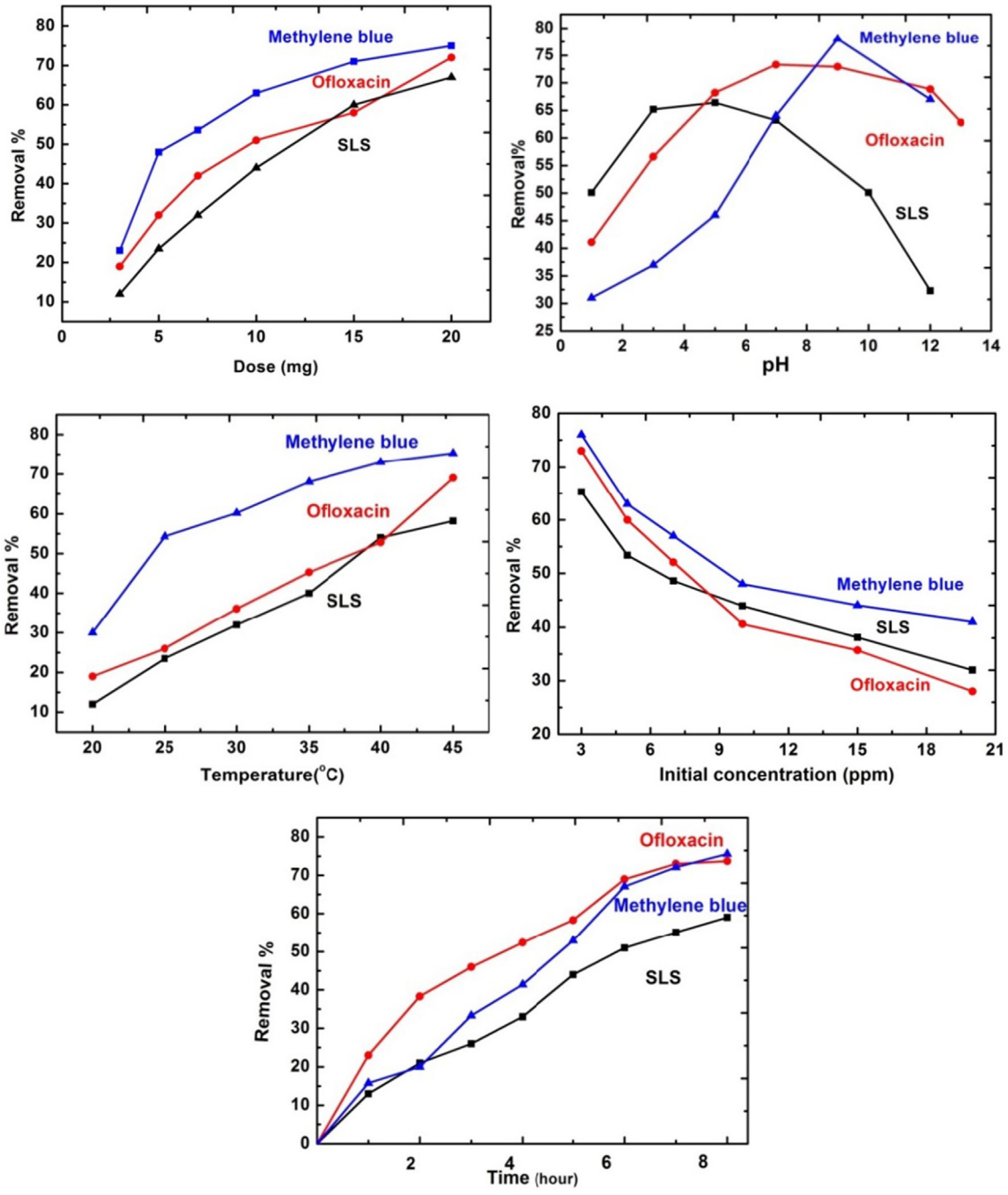

Fig. 5. Factors affecting the adsorption process.

the drug was between 4 and 9. The anionic surfactant SLS possess a negative charge on their hydrophilic end. The best removal results were from acidic to quite a neutral medium of pH (3–6) due to the availability of positive charged adsorption active sites, which decreased by increasing the pH by more than 7. For the three applications, the uptake of the pollutants was enhanced when the temperature increased from 20 to 45 °C, due to the chemical reaction between the contaminants and the adsorbent surfaces and due to the increasing intraparticle diffusion of adsorbate ions between adsorbent pores by rising of temperature reflecting endothermic adsorption process. The adsorption efficiency increased directly with time till saturation of the surface adsorption sites and reached some stability due to the equilibrium between adsorbent and adsorbate. The removal efficiency decreased with the increasing initial concentration of pollutants due to the insufficient active sites for adsorption, and hence the removal activity decreased.

For the three applications, when comparing removal results carried out by TiO_2 and zinc-doped TiO_2 nanoparticles in the best conditions, there are more enhancements to the adsorption efficiency for the modified nanoparticles. The modified nanoparticles Zn doped-TiO_2 gave a more successful outcome as seen from Figure (6) and more adsorption activity than TiO_2 overall affecting factors due to better surface properties for modified nanoparticles with higher surface area and better porosity more available variables pore sizes as active adsorption sites.

3.2.2. *Behavior and mechanism of adsorption of zinc-doped TiO_2*

The analysis results by BET revealed the enhancement of the surface properties of TiO_2 by zinc doping, as illustrated in Table 2. XRD data prove the positive impact of zinc doping due to the synthesis of smaller nanoparticles and the incorporation of zinc ions of smaller ionic radii in the TiO_2 crystal lattice, which results in lattice distortion. The difference in the coordination between Ti^{4+}, Zn^{2+} causes the availability of free electrons at the nanoparticle surface, which enhances the adsorption ability of doped nanoparticles. The pH factor has a special role in controlling the adsorption

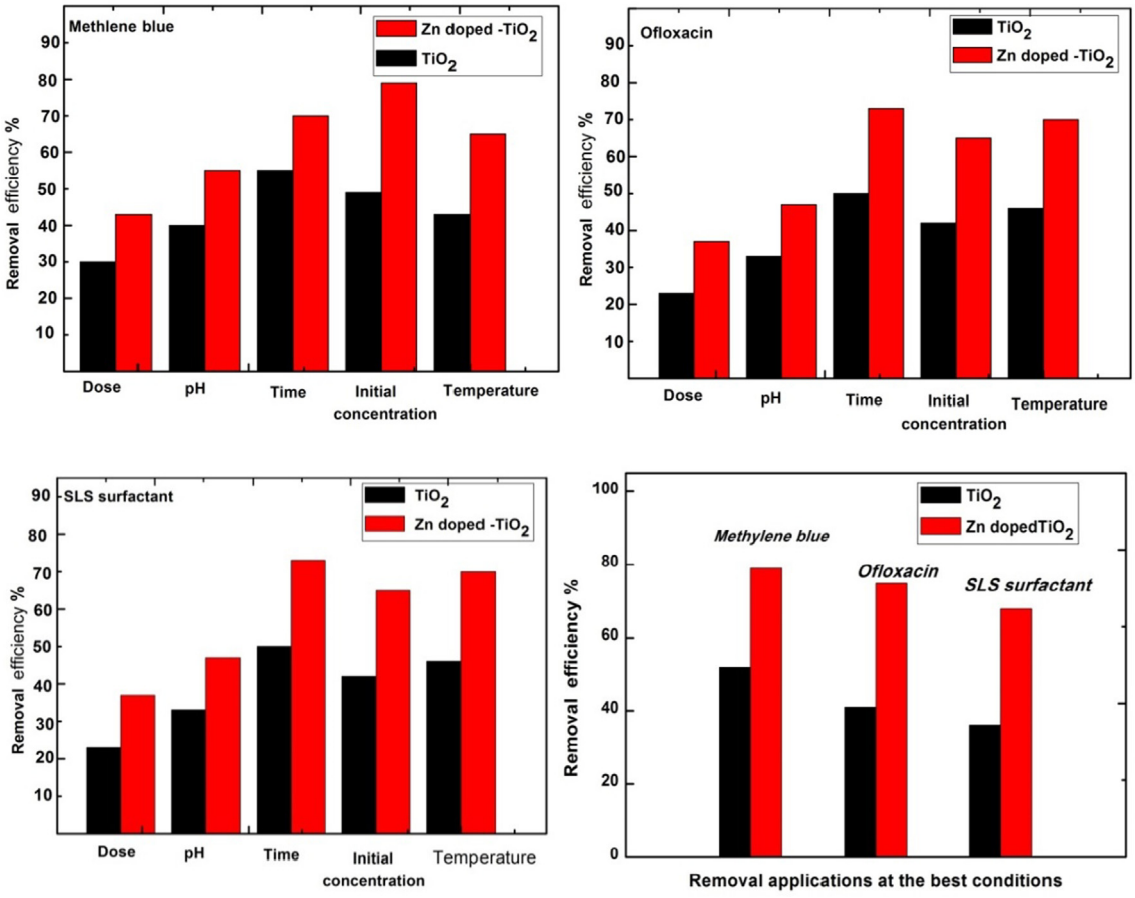

Fig. 6. The removal efficiency of TiO_2, Zn doped -TiO_2 over different factors.

process. At lower pH than 5 the availability of H^+ and protonated active sites tend to adsorption of anionic SLS and repulsion with cationic species (methylene blue). Higher pH values of more than 8 cause the depletion of protons in addition to the deprotonation of hydroxyl groups on nanoparticle surfaces and better adsorption of methylene blue. Ofloxacin chemical composition is characterized by anionic and cationic groups in its chemical structure, which reflect the possible adsorption in a wide pH range. The negative charge of the TiO_2 and the presence of positive zinc sites gave the diversity of doped nanoparticle surface and the ability of adsorption of methylene blue cationic dye and SLS anionic surfactant and ofloxacin drug.

3.3. Effect of the interfering species on the adsorption efficiency

For examining the effect of the interfering species, the interfering pollutant should have a higher concentration (about 50 fold) to have the interfering effect on the value of absorption of the dye, drug, and the surfactant by UV spectrophotometer by which the absorbance was taken without and with each of the interfering material taking in consideration that the initial value of absorbance were 0.657, 1.74 and 0.124 for 10 ppm methylene blue, 10 ppm ofloxacin, and 200 ppm SLS detergent respectively. The interfering species were "glucose, TiO_2, KCl, Diclofenac sodium, ammonium salt, lead acetate, and CTAB and the results were summarized in Table 3.

3.4. Adsorption isotherm for methylene blue, ofloxacin, and detergent

The efficiency of adsorption depends on the chemical and physical properties of the adsorbents. This work studied different adsorption isotherms (Langmuir, Freundlich, and Temkin) for pollutants on the surface of modified TiO_2.

3.4.1. Langmuir adsorption isotherm

Langmuir's adsorption isotherm model studies the coverage of the surface of the adsorbent with maximum adsorption capacity (Q_{max}) by homogeneous monolayers on identical equivalent active sites in a simple system [60,61].

The values *of QE* and Q_{max} are the amount of adsorbates at equilibrium and a maximum monolayer adsorption capacity (mg/g), respectively, can be calculated from equation (2):

$$\frac{1}{q_e} = \frac{1}{q_{max}} + \frac{1}{q_{max} k_L C_e} \tag{2}$$

where C_e is the concentration of the adsorbates at equilibrium (mg/L) and K_L is the Langmuir adsorption constant. The values of q_{max} and k_L can be calculated from the graph between $1/q_e$ and $1/C_e$ through the slope and intercept as in Table 4 and Fig. 7.

3.4.2. Freundlich adsorption isotherm model

Freundlich adsorption isotherm can be applied to study adsorption at heterogeneous surfaces [61–64]. Q_e is the adsorbed pollutant per gram of the adsorbent at equilibrium (mg/g) that can be represented from equation 3:

$$Log\ Q_e = Log\ K_f + 1/n\ Log\ C_e \tag{3}$$

where K_f is the Freundlich isotherm constant (mg/g), n is the adsorption intensity, and C_e is the equilibrium concentration of adsorbates (mg/L).

The K_f constant value is considered an approximate indicator of adsorption capacity. When n is equal to 1, the partition between the two phases is independent of concentration. The values of 1/n, K_f can be calculated from the slopes and intercepts of the previous curves as in table (4) and Fig. 7.

3.4.3. Temkin adsorption isotherm model

Temkin adsorption isotherm assumes that the energy of adsorption for molecules decreases

Table 3. The effect of the interfering species on the adsorption efficiency.

Interfering Components	M.B.	Interfering effect %	Ofloxacin	Interfering effect %	SLS	Interfering effect %
None	0.657	....	1.74	....	0.124	....
Glucose	0.616	6.24	1.741	....	0.123	0.8
Diclofenac sodium	0.613	6.7	1.734	0.34	0.120	3.2
KCl	0.631	3.96	1.748	....	0.129	....
TiO_2	0.564	14.1	1.685	3.2	0.114	8.1
CTAB	0.653	0.6	1.738	0.11	0.123	0.8
NH_4^+	0.655	0.3	1.739	0.1	0.124	....
Lead acetate	0.651	0.9	1.736	0.22	0.122	1.6
Methylene blue	0.66	....	1.735	0.25	0.12	3.2
Ofloxacin	0.657	....	1.741	....	0.122	1.6
SLS	0.656	0.1	1.739	0.1	0.124	....

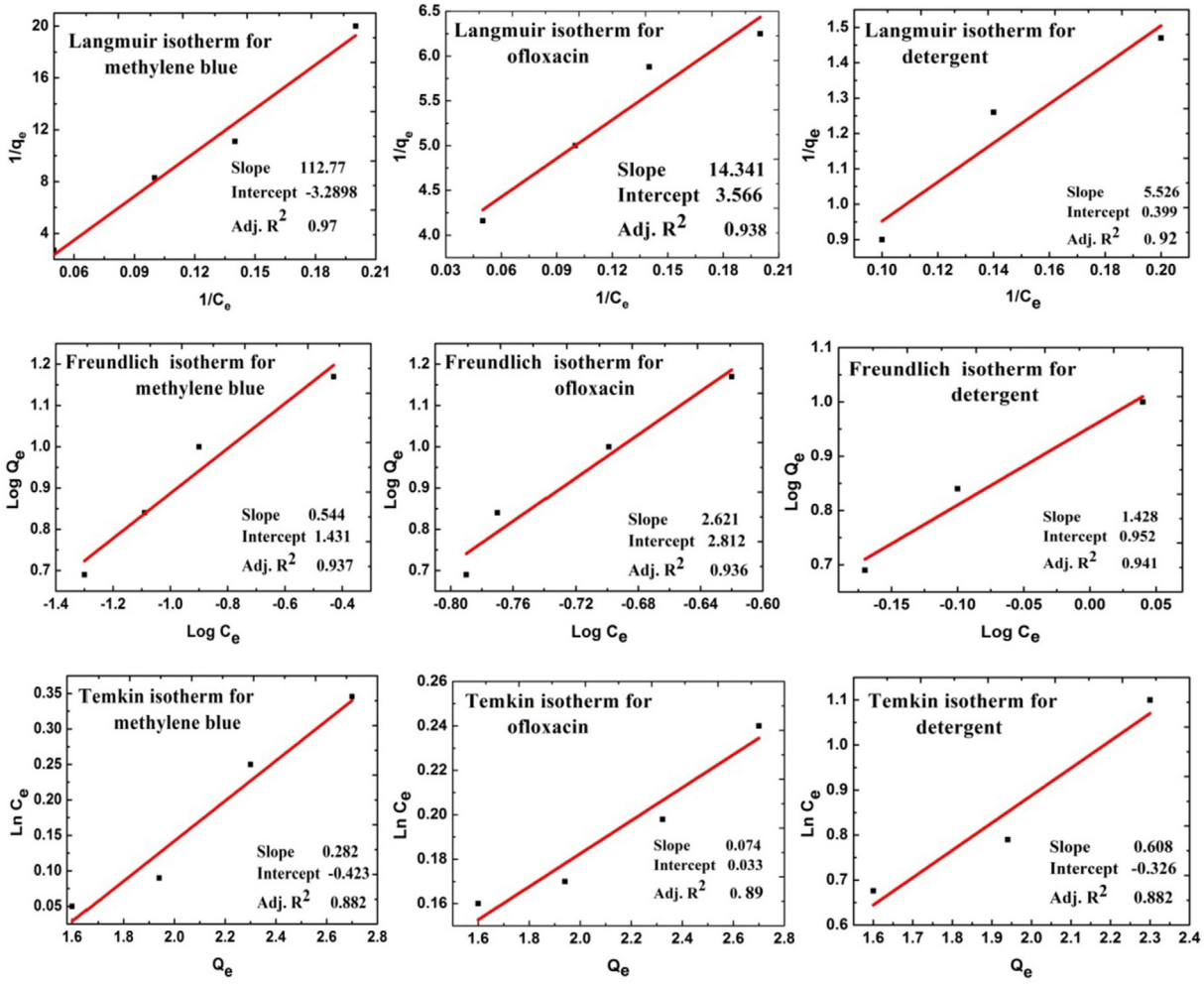

Fig. 7. Isotherm curves for the three pollutants.

linearly with increasing the coverage of the surface of the adsorbent due to the adsorbate–adsorbent interaction. Temkin also assumes that distribution is characterized by uniformity up to maximum binding energy [63,64]. The following equation (4) can describe the Temkin isotherm model:

$$Q_e = B\ Ln\ A + B\ Ln\ C_e \quad (4)$$

where: Q_e: is the metal adsorbed in mg/gram of adsorbent, C_e is the concentration of the adsorbates at equilibrium in ppm. The value of A is the equilibrium binding constant, and B is a constant related to the heat of sorption, which is equal to $B = RT/b_T$. Where R is the ideal gas constant (8.314 J mol^{-1} K^{-1} and b_T is

Table 4. Parameters of variable isotherms.

Parameter		Methylene blue	Ofloxacin	Detergent
Langmuir isotherm	Q_{max}	9.304	11.28	7.5
	K_L	0.025	0.249	0.172
	R^2	0.97	0.938	0.92
Freundlich isotherm	*1/n*	0.54	2.62	1.42
	N	1.85	0.28	0.7
	K_f	1.43	2.81	0.92
	R^2	0.937	0.93	0.941
Temkin isotherm	*A*	5.073	4.021	3.51
	B	0.33	0.21	0.137
	R^2	0.882	0.89	0.88

Table 5. Removal results of pollutants from synthetic samples.

Sample code	Methylene blue			Ofloxacin			SLS		
	C_o (mg/L)	C_e (mg/L)	R%	C_o (mg/L)	C_e (mg/L)	R%	C_o (mg/L)	C_e (mg/L)	R%
1	*9.34*	*2.92*	68.7	*3.16*	*3.16*	65.1	*50.1*	*21.1*	57.8
2	*5.97*	*1.24*	79.3	*4.47*	*4.47*	63.0	*28.4*	*10.2*	64.0
3	*4.83*	*1.1*	77.2	*2.66*	*2.66*	47.3	*45.3*	*20.4*	55.0
4	*3.81*	*1.22*	67.9	*1.84*	*1.84*	37.5	*33.2*	*14.2*	57.2
5	*2.89*	*1.01*	65.0	*4.13*	*4.13*	76.9	*25.8*	*17.6*	68.2
6	2.12	1.52	28.3	4.55	1.93	57.5	44.1	13.6	69.1
7	3.42	1.24	63.7	3.21	1.66	48.2	23.2	10.2	48.4
8	2.51	1.22	51.3	6.44	2.22	65.5	36.2	14.1	38.9
9	3.14	1.63	48.0	5.21	2.35	54.8	39.3	15.4	60.7
10	1.96	1.2	38.7	3.45	1.24	64.0	47.9	12.9	73.0

the Temkin isotherm constant), Temkin parameters can be determined from the Qe vs. log Ce graph.

All parameters of variable isotherms Langmuir, Freundlich and Temkin are summarized in Table 4 and Fig. 7. In both models of adsorption isotherms Langmuir and Freundlich, it was noticed that the straight lines and higher values of R^2 than that obtained by the Temkin equation indicated heterogeneous adsorption on the surface of the adsorbent but at many equivalent active sites. That explains the adsorption behavior fitted with Langmuir and Freundlich equations than Temkin isotherm.

3.5. Practical applications on water samples

For the potential application of Zn doped -TiO_2 nanoparticles in the treatment of some synthetic polluted water samples. New stock solutions of pollutants (methylene blue 10 ppm, ofloxacin 7 ppm, and SLS 50 ppm) have been prepared and diluted with water in different amounts to obtain ten different concentrations (C_o) of pollutant mixture which have been treated with nanoparticles by mixing and vigorous stirring.

The initial concentrations and at equilibrium (C_o, C_e) were determined according to the absorption reading with removal % (R %) calculation. The results which were summarized in Table 5 show that the cationic dye, quinolone antibiotic (ofloxacin), and detergent (SLS) were effectively adsorbed on the surface of modified Zn/TiO_2 nanomaterial, reflecting its applicability and high performance in the removal of organic compounds from the wastewater by great amounts exceeded 75% for each, inhibiting their accumulation and subsequent dangerous environmental side effects and free of consumed energy.

3.6. Advantages and the reusability of Zn doped TiO_2

The modified nanoparticles were characterized by their easy preparation procedure; very low cost, available raw materials in addition to very small required amounts with high removal activity for variable pollutants.

After each adsorption application, the nanoparticles can be washed by ethanol several times and employed for another adsorption treatment for about 2–3 cycles, but with descending of their activity due to repeated removal processes as shown in Figure (8).

3.7. Adsorption efficiency comparison with other works

Many adsorption studies have been established using various adsorbents to remove different pollutants, such as methylene blue ofloxacin and SLS.

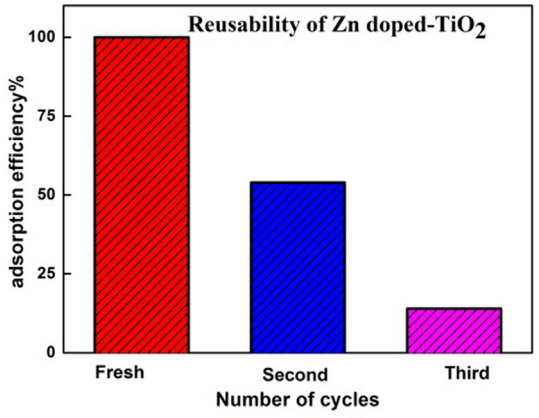

Fig. 8. Reusability of Zn doped TiO_2.

Table 6. Comparison for different pollutant removal by variable adsorbents.

Adsorbent	Pollutant	Q_{max} (mg/g)	Ref
Wood millet carbon	dye	4.9	[53]
Non porous SiO_2	Ofloxacin	2.1	72
Apricot stones	dye	4.1	68
GO/SA	ofloxacin	1.798	72
Zn doped TiO_2	ofloxacin	11.23	This work
Neem saw dust	dye	3.6	71
Zn doped TiO_2	dye	9.3	This work
Met-GO/SA	ofloxacin	3.436	72
TiO_2	SLS	3.25	This work
Wall nut shells	dye	4.1	68
TiO_2	Ofloxacin	8.3	This work
Beer brewery waste	dye	4.92	71
Rice halls	dye	3.92	68
Zn doped TiO_2	SLS	7.5	This work

Their maximum adsorption results (Q_{max}) were summarized in Table 6. Many of these adsorbents have higher costs and are less active than our modified nanoparticles, characterized by their low cost-benefit with simple and rapid application in ambient conditions [35,50,65].

4. Conclusion

The study reflects a positive impact on the importance of the modified zinc doped TiO2 nanoparticles in wastewater treatment by adsorption. The successful doping of anatase TiO_2 by zinc species affects the crystal particle sizes to a smaller range of (19–25 nm) and increases the surface area to be $26 m^2 g^{-1}$. The modified zinc doped TiO_2 nanoparticles have high adsorption activity in wastewater treatment with excellent removal results, 75.1%, 71.1%, and 68.2% for adsorption of methylene blue, ofloxacin, and SLS, respectively, in synthetic samples without any required energy or subsequent pollution. The adsorption behavior was better discussed by Langmuir and Freundlich isotherm models than Temkin isotherm according to the R^2 correlation coefficient. The modified nanomaterial is characterized by its good regeneration and reusability for about 2–3 cycles. The removal of different contaminants from wastewater via modified Zn-doped TiO_2 nanoparticles by adsorption can be considered as an effortless, low-cost, and clean process without the need for complex toxic chemicals or consumed energy.

Funding

The present work is self-funding.

Data availability

Not applicable.

Conflict of interest

The authors declare no competing interests.

References

[1] Jian-Ping Zou, Hui-Long Liu, Jinming Luo, Qiu-Ju Xing, Hong-Mei Du, Xun-Heng Jiang, Xu-Biao Luo, Sheng-Lian Luo, Steven L. Suib, Three-dimensional reduced graphene oxide coupled with Mn_3O_4 for highly efficient removal of Sb (III) and Sb (V) from water, ACS Appl Mater Interfaces 8 (2016) 18140–18149.
[2] S.-S. Liu, C.-K. Lee, H.-C. Chen, C.-C. Wang, L.-C. Juang, Application of titanate nanotubes for Cu (II) ions adsorptive removal from aqueous solution, Chem Eng J 147 (2009) 188–193.
[3] P. Goh, B. Ng, W. Lau, A. Ismail, Inorganic nanomaterials in polymeric ultrafiltration membranes for water treatment, Separ Purif Rev 44 (2015) 216–249.
[4] J.-H. Kim, K.-K. Oh, S.-T. Lee, S.-W. Kim, S.-I. Hong, Biodegradation of phenol and chlorophenols with defined mixed culture in shake-flasks and a packed bed reactor, Process Biochem 37 (2002) 1367–1373.
[5] M.D. Adjei, T.M. Heinze, J. Deck, J.P. Freeman, A.J. Williams, J.B. Sutherland, Transformation of the antibacterial agent norfloxacin by environmental mycobacteria, Appl Environ Microbiol 72 (2006) 5790–5793.
[6] A.V. Herrera-Herrera, J. Hernández-Borges, T.M. Borges-Miquel, M.A. Rodriguez-Delgado, Dispersive liquid–liquid microextraction combined with nonaqueous capillary electrophoresis for the determination of fluoroquinolone antibiotics in waters, Electrophoresis 31 (2010) 3457–3465.
[7] I. Michael, L. Rizzo, C.S. McArdell, C.M. Manaia, C. Merlin, T. Schwartz, C. Dagot, D. Fatta-Kassinos, Urban wastewater treatment plants as hotspots for the release of antibiotics in the environment: a review, Water Res 47 (2013) 957–995.
[8] M. Sui, S. Xing, L. Sheng, S. Huang, H. Guo, Heterogeneous catalytic ozonation of ciprofloxacin in water with carbon nanotube supported manganese oxides as catalyst, J Hazard Mater 227 (2012) 227–236.
[9] X. Hu, Q. Zhou, Y. Luo, Occurrence and source analysis of typical veterinary antibiotics in manure, soil, vegetables and

groundwater from organic vegetable bases, northern China, Environ Pollut 158 (2010) 2992–2998.
[10] X.X. Zhang, L.L. Dong, K. Cai, R.P. Li, A routine method for simultaneous determination of three classes of antibiotics in aquaculture water by SPE-RPLC-UV, in: Advanced materials research, Trans Tech Publ, 2013, pp. 1253–1259.
[11] B. Dewitte, J. Dewulf, K. Demeestere, V. Van De Vyvere, P. De Wispelaere, H. Van Langenhove, Ozonation of ciprofloxacin in water: HRMS identification of reaction products and pathways, Environ Sci Technol 42 (2008) 4889–4895.
[12] E. De Bel, J. Dewulf, B. De Witte, H. Van Langenhove, C. Janssen, Influence of pH on the sonolysis of ciprofloxacin: biodegradability, ecotoxicity and antibiotic activity of its degradation products, Chemosphere 77 (2009) 291–295.
[13] G. Lofrano, M. Carotenuto, C.S. Uyguner-Demirel, A. Vitagliano, A. Siciliano, M. Guida, An integrated chemical and ecotoxicological assessment for the photocatalytic degradation of vancomycin, Environ Technol 35 (2014) 1234–1242.
[14] A. Fakhri, M. Naji, S. Tahami, Ultraviolet/ultrasound-activated persulfate for degradation of drug by zinc selenide quantum dots: catalysis and microbiology study, J Photochem Photobiol B Biol 170 (2017) 304–308.
[15] Li-Jun Zhou, Guang-Guo Ying, Shan Liu, Jian-Liang Zhao, Feng Chen, Rui-Quan Zhang, Fu-Qiang Peng, Qian-Qian Zhang, Simultaneous determination of human and veterinary antibiotics in various environmental matrices by rapid resolution liquid chromatography–electrospray ionization tandem mass spectrometry, J Chromatogr A 1244 (2012) 123–138.
[16] P. Martins, R. Miranda, J. Marques, C.J. Tavares, G. Botelho, S. Lanceros-Mendez, Comparative efficiency of TiO2 nanoparticles in suspension vs. immobilization into P (VDF–TrFE) porous membranes, RSC Adv 6 (2016) 12708–12716.
[17] Michela Sturini, Andrea Speltini, Federica Maraschi, Antonella Profumo, Luca Pretali, Elisa Fasani, Angelo Albini, Photochemical degradation of marbofloxacin and enrofloxacin in natural waters, Environ Sci Technol 44 (2010) 4564–4569.
[18] J.A. de Lima Perini, M. Perez-Moya, R.F.P. Nogueira, Photo-Fenton degradation kinetics of low ciprofloxacin concentration using different iron sources and pH, J Photochem Photobiol Chem 259 (2013) 53–58.
[19] C. Liu, V. Nanaboina, G.V. Korshin, W. Jiang, Spectroscopic study of degradation products of ciprofloxacin, norfloxacin and lomefloxacin formed in ozonated wastewater, Water Res 46 (2012) 5235–5246.
[20] C.A. Fogarty, Photocatalytic oxidation of Ciprofloxacin under UV-LED light, 2013.
[21] C. Pablos, J. Marugan, R. van Grieken, E. Serrano, Emerging micropollutant oxidation during disinfection processes using UV-C, UV-C/H_2O_2, UV-A/TiO_2 and UV-A/TiO_2/H_2O_2, Water Res 47 (2013) 1237–1245.
[22] S. Teixeira, R. Gurke, H. Eckert, K. Kühn, J. Fauler, G. Cuniberti, Photocatalytic degradation of pharmaceuticals present in conventional treated wastewater by nanoparticle suspensions, J Environ Chem Eng 4 (2016) 287–292.
[23] T.A. Gad-Allah, M.E. Ali, M.I. Badawy, Photocatalytic oxidation of ciprofloxacin under simulated sunlight, J Hazard Mater 186 (2011) 751–755.
[24] G.-G. Ying, Fate, behavior and effects of surfactants and their degradation products in the environment, Environ Int 32 (2006) 417–431.
[25] A.K. Mungray, P. Kumar, Fate of linear alkylbenzene sulfonates in the environment: a review, Int Biodeterior Biodegrad 63 (2009) 981–987.
[26] V. Ochoa-Herrera, R. Sierra-Alvarez, Removal of perfluorinated surfactants by sorption onto granular activated carbon, zeolite and sludge, Chemosphere 72 (2008) 1588–1593.
[27] G. Busca, S. Berardinelli, C. Resini, L. Arrighi, Technologies for the removal of phenol from fluid streams: a short review of recent developments, J Hazard Mater 160 (2008) 265–288.
[28] D. Berryman, F. Houde, C. DeBlois, M. O'Shea, Nonylphenolic compounds in drinking and surface waters downstream of treated textile and pulp and paper effluents: a survey and preliminary assessment of their potential effects on public health and aquatic life, Chemosphere 56 (2004) 247–255.
[29] S. Khan, C. Chao, M. Waqas, H.P.H. Arp, Y.-G. Zhu, Sewage sludge biochar influence upon rice (Oryza sativa L) yield, metal bioaccumulation and greenhouse gas emissions from acidic paddy soil, Environ Sci Technol 47 (2013) 8624–8632.
[30] S.J. Flora, G. Flora, G. Saxena, Environmental occurrence, health effects and management of lead poisoning, in: Lead, Elsevier, 2006, pp. 158–228.
[31] P.Z. Si, W. Jiang, H.X. Wang, Z.F. Li, J.J. Liu, J.G. Lee, C.J. Choi, Large scale synthesis of nitrogen doped TiO_2 nanoparticles by reactive plasma, Mater Lett 68 (2012) 161–163.
[32] C.K. Ahn, D. Park, S.H. Woo, J.M. Park, Removal of cationic heavy metal from aqueous solution by activated carbon impregnated with anionic surfactants, J Hazard Mater 164 (2009) 1130–1136.
[33] P. Dhandapani, S. Maruthamuthu, G. Rajagopal, Bio-mediated synthesis of TiO_2 nanoparticles and its photocatalytic effect on aquatic biofilm, J Photochem Photobiol B Biol 110 (2012) 43–49.
[34] M.S. Tehrani, R. Zare-Dorabei, Competitive removal of hazardous dyes from aqueous solution by MIL-68 (Al): derivative spectrophotometric method and response surface methodology approach, Spectrochim Acta Mol Biomol Spectrosc 160 (2016) 8–18.
[35] F. Salimi, H. Rahimi, C. Karami, Removal of methylene blue from water solution by modified nanogoethite by Cu, Desalination Water Treat 137 (2019) 334–344.
[36] B. Debnath, M. Majumdar, M. Bhowmik, K.L. Bhowmik, A. Debnath, D.N. Roy, The effective adsorption of tetracycline onto zirconia nanoparticles synthesized by novel microbial green technology, J Environ Manag 261 (2020) 110235.
[37] I. Elmehasseb, S. Kandil, K. Elgendy, Advanced visible-light applications utilizing modified Zn-doped TiO_2 nanoparticles via non-metal in situ dual doping for wastewater detoxification, Optik (2020) 164654.
[38] K. Elgendy, I. Elmehasseb, S. Kandil, Synthesis and characterization of rare earth metal and non-metal co-doped TiO_2 nanostructure for photocatalytic degradation of Metronidazole, Environment 10 (2019) 60–67.
[39] K. Shoueir, S. Kandil, H. El-hosainy, M. El-Kemary, Tailoring the surface reactivity of plasmonic Au@ TiO_2 photocatalyst bio-based chitosan fiber towards cleaner of harmful water pollutants under visible-light irradiation, J Clean Prod 230 (2019) 383–393.
[40] W. Wang, S. Li, C. Pan, S. Liu, T. Luo, G. Dai, Template-free fabrication of ZnS/TiO_2 photocatalyst with macrochannels, J Chin Chem Soc 65 (2018) 252–258.
[41] Milan Králik, Adsorption, chemisorption, and catalysis, Chem Pap 68 (2014) 1625–1638.
[42] B. Dong, T. Liu, C. Li, F. Zhang, Species, engineering and characterizations of defects in TiO_2-based photocatalyst, Chin Chem Lett 29 (2018) 671–680.
[43] R. Begum, J. Najeeb, A. Sattar, K. Naseem, A. Irfan, A.G. Al-Sehemi, Z.H. Farooqi, Chemical reduction of methylene blue in the presence of nanocatalysts: a critical review, Rev Chem Eng 36 (2020) 749–770.
[44] P. Das, P. Debnath, A. Debnath, Enhanced sono-assisted adsorptive uptake of malachite green dye onto magnesium ferrite nanoparticles: kinetic, isotherm and cost analysis, Environ Nanotechn Monit Manag 16 (2021) 100506.
[45] D. Raoufi, T. Raoufi, The effect of heat treatment on the physical properties of sol–gel derived ZnO thin films, Appl Surf Sci 255 (2009) 5812–5817.

[46] V. Vetrivel, K. Rajendran, V. Kalaiselvi, Synthesis and characterization of pure titanium dioxide nanoparticles by sol-gel method, Int J Chem Res 7 (2015) 1090–1097.
[47] M.R.M. Shafiee, M.P. Zakaria, P.A. Azar, Aluminum tris (dihydrogen phosphate)[Al(H2PO 4) 3] as an efficient and heterogeneous catalyst for the environmentally friendly preparation of N, N′-alkylidene biscarbamates, in: 2010 2nd international conference on chemical, biological and environmental engineering, IEEE, 2010, pp. 168–171.
[48] Rasel Das, Chad D. Vecitis, Agnes Schulze, Bin Cao, Ahmad Fauzi Ismai, Xianbo Lu, Jiping Chen, Seeram Ramakrishna, Recent advances in nanomaterials for water protection and monitoring, Chem Soc Rev 46 (2017) 6946–7020.
[49] S.H. Mosavi, R. Zare-Dorabei, M. Bereyhi, Rapid and effective ultrasonic-assisted adsorptive removal of Congo red onto MOF-5 modified by $CuCl_2$ in ambient conditions: adsorption isotherms and kinetics studies, ChemistrySelect 6 (2021) 4432–4439.
[50] M.S. Tehrani, R. Zare-Dorabei, Highly efficient simultaneous ultrasonic-assisted adsorption of methylene blue and rhodamine B onto metal organic framework MIL-68 (Al): central composite design optimization, RSC Adv 6 (2016) 27416–27425.
[51] A. Deb, A. Debnath, B. Saha, Ultrasound-aided rapid and enhanced adsorption of anionic dyes from binary dye matrix onto novel hematite/polyaniline nanocomposite: response surface methodology optimization, Appl Organomet Chem 34 (2020), e5353.
[52] T.J. Al-Musawi, G. McKay, P. Rajiv, N. Mengelizadeh, D. Balarak, Efficient sonophotocatalytic degradation of acid blue 113 dye using a hybrid nanocomposite of $CoFe_2O_4$ nanoparticles loaded on multi-walled carbon nanotubes, J Photochem Photobiol Chem 424 (2022) 113617.
[53] T.J. Al-Musawi, N. Mengelizadeh, K. Sathishkumar, S. Mohebi, D. Balarak, Preparation of $CuFe_2O_4$/montmorillonite nanocomposite and explaining its performance in the sonophotocatalytic degradation process for ciprofloxacin, Coll Interf Sci Commun 45 (2021) 100532.
[54] D. Balarak, N. Mengelizadeh, P. Rajiv, K. Chandrika, Photocatalytic degradation of amoxicillin from aqueous solutions by titanium dioxide nanoparticles loaded on graphene oxide, Environ Sci Pollut Control Ser (2021) 1–12.
[55] T.J. Al-Musawi, P. Rajiv, N. Mengelizadeh, I.A. Mohammed, D. Balarak, Development of sonophotocatalytic process for degradation of acid orange 7 dye by using titanium dioxide nanoparticles/graphene oxide nanocomposite as a catalyst, J Environ Manag 292 (2021) 112777.
[56] T.J. Al-Musawi, P. Rajiv, N. Mengelizadeh, F.S. Arghavan, D. Balarak, Photocatalytic efficiency of $CuNiFe_2O_4$ nanoparticles loaded on multi-walled carbon nanotubes as a novel photocatalyst for ampicillin degradation, J Mol Liq 337 (2021) 116470.
[57] A. Deb, A. Debnath, N. Bhattacharjee, B. Saha, Ultrasonically enhanced dye removal using conducting polymer functionalised ZnO nanocomposite at near neutral pH: kinetic study, isotherm modelling and adsorbent cost analysis, Int J Environ Anal Chem (2020) 1–20.
[58] S. Nourozi, R. Zare-Dorabei, Highly efficient ultrasonic-assisted removal of methylene blue from aqueous media by magnetic mesoporous silica: experimental design methodology, kinetic and equilibrium studies, Desalination Water Treat 85 (2017) 184–196.
[59] M. Roosta, M. Ghaedi, A. Asfaram, Simultaneous ultrasonic-assisted removal of malachite green and safranin O by copper nanowires loaded on activated carbon: central composite design optimization, RSC Adv 5 (2015) 57021–57029.
[60] S. Bingham, W.A. Daoud, Recent advances in making nano-sized TiO_2 visible-light active through rare-earth metal doping, J Mater Chem 21 (2011) 2041–2050.
[61] A.S. Thajeel, Isotherm, kinetic and thermodynamic of adsorption of heavy metal ions onto local activated carbon, Aquat Sci Technol 1 (2013) 53–77.
[62] M.B. Ibrahim, S. Sani, Comparative isotherms studies on adsorptive removal of Congo red from wastewater by watermelon rinds and neem-tree leaves, Open J Phys Chem 4 (2014) 139.
[63] A. Dada, A. Olalekan, A. Olatunya, O. Dada, Langmuir, Freundlich, Temkin and Dubinin–Radushkevich isotherms studies of equilibrium sorption of Zn^{2+} unto phosphoric acid modified rice husk, IOSR J Appl Chem 3 (2012) 38–45.
[64] M.D.G. de Luna, E.D. Flores, D.A.D. Genuino, C.M. Futalan, M.-W. Wan, Adsorption of Eriochrome Black T (EBT) dye using activated carbon prepared from waste rice hulls—optimization, isotherm and kinetic studies, J Taiwan Inst Chem Eng 44 (2013) 646–653.
[65] S. Naeem, V. Baheti, J. Militky, J. Wiener, P. Behera, A. Ashraf, Sorption properties of iron impregnated activated carbon web for removal of methylene blue from aqueous media, Fibers Polym 17 (2016) 1245–1255.